

Unraveling quinoproteins-based extracellular electron transport in humus-dependent respiratory growth of *Methanosarcina acetivorans*

Yuanxu Song

Shandong university

Ling Li

Shandong university

Kaifeng Du

Shandong university

Fanping Zhu

Shandong university

Chao Song

Shandong university

Xian-Zheng Yuan

Shandong University <https://orcid.org/0000-0002-7893-0692>

Mingyu Wang

Shandong University <https://orcid.org/0000-0003-1215-9556>

Shuguang Wang

Shandong university

James G. Ferry

Pennsylvania State University

Zhen Yan (✉ yanzhen@email.sdu.edu.cn)

Shandong University <https://orcid.org/0000-0002-6213-9054>

Article

Keywords:

Posted Date: April 19th, 2022

DOI: <https://doi.org/10.21203/rs.3.rs-1562983/v1>

License:   This work is licensed under a Creative Commons Attribution 4.0 International License.

[Read Full License](#)

Abstract

Microbial respiration using humus plays a critical role in organic matter decomposition and biogeochemical cycling of elements in diverse natural environments. A longstanding recognition is that microbial respiration is achieved through extracellular electron transfer mediated by electrical pili or *c*-type cytochromes. Here, we describe the capability of humus-dependent respiratory growth of a methanogen, namely *Methanosarcina acetivorans*, which is a model for studying acetoclastic methanogenesis. A previously unexplored gene cluster that encodes cell surface quinoproteins was identified as being responsible for extracellular electron transfer. Pyrroloquinoline quinone was found to be a cofactor for the quinoproteins, providing electrical interplay sites with quinone moieties of humus. The membrane-bound methanophenazine, which is analogous to ubiquinone, participated in extracellular electron transfer, being potentially coupled with energy-conserving humus respiration. Given that these quinoproteins are widely distributed in methanogens, our findings extend the current understanding of microbial humus respiration in the context of global methane dynamics.

Introduction

Humic substances, also called humus, constitute the highly transformed fraction of natural organic matter that is derived from the residues of dead organisms and their degradation products. Humus are present across terrestrial and aquatic environments including soil, wetlands and marine environments and represent a significant carbon pool over a range of biospheres. Humus were long considered to be inert to biodegradation because of their heterogeneous structures and amorphous compositions. However, humus display versatile reactivities with a diverse suite of organic compounds and minerals through both biotic and abiotic processes. Specifically, microbial humus respiration is a ubiquitous process that significantly impacts organic matter decomposition and the biogeochemical cycling of key elements in natural environments^{1,2}.

The study of humus respiration began two decades ago, when Dr. Lovley and coworkers showed that *Geobacter* and *Shewanella* from soil and freshwater sediments reduced humus, yielding energy to support their growth³. Subsequently, they found that humus could also serve as an electron shuttle for humus-reducing microbes to reduce other insoluble electron acceptors⁴. The quinone groups in humus are the primary electron-accepting moieties, as evidenced by the accumulation of semiquinones as the main radicals during this metabolism⁵. The electrically conductive pili (*e*-pili) and outer-membrane multiheme *c*-type cytochromes (MHCs) of humus-reducing microbes are critical components of extracellular electron transfer⁶. Furthermore, reduced humus could also donate electrons to humus-reducing microbes, a process that is mediated by quinone moieties in humus and *e*-pili or MHCs in microbes⁷. The anaerobic redox cycling of humus in sedimentary environments can facilitate the abiotic reduction of less accessible electron acceptors, such as insoluble Fe or Mn oxides, which thereby influences their biogeochemical transformation and speciation⁸. In addition, the redox cycling of humus can enhance the organic matter oxidation rates in diverse biospheres and may potentially play a

regulatory role in the emission of greenhouse gases such as CO₂ and methane, making it ecologically important for global carbon cycling^{9,10}.

Methanosarcina spp., which belong to methanogenic archaea, are another type of microbe that may be able to respire humus for growth because of their ability to perform extracellular electron transfer^{11–14}. *Methanosarcina* spp. inhabit most natural and engineered anaerobic ecosystems and have tremendous metabolic flexibility. They are capable of acetoclastic (acetate), hydrogenotrophic (CO₂/H₂), methylotrophic (methanol/methylamines) and methyl-reducing (H₂ and methanol/methylamines) methanogenesis¹¹. Electrons are generated intracellularly from methanogenesis and are transferred to a membrane-bound electron transport chain in the reduced form of ferredoxin (Fd_{red}) and cofactor F₄₂₀ (F₄₂₀H₂). *Methanosarcina* spp. employs versatile electron transport chains to obtain energy for growth. For H₂-utilizing species, such as *M. barkeri* and *M. mazei*, intracellular electrons are donated to a membrane-bound Ech hydrogenase, which induces H₂ cycling with another membrane-bound Vho hydrogenase, where proton gradient is generated¹⁵. For H₂-independent species that lack Ech and Vho hydrogenases, such as *M. acetivorans*, Fd_{red} and F₄₂₀H₂ donate electrons to the membrane-bound *Rhodobacter* nitrogen fixation (Rnf) and F₄₂₀H₂ dehydrogenase (Fpo) complexes, respectively, and create proton and sodium gradients for energy conservation^{16,17}. Methanophenazine (MP), which is a membrane-bound electron carrier analogous to ubiquinone, mediates the transfer of electrons from membrane-bound hydrogenases or complexes to an intracellular terminal electron acceptor, namely, CoMS-SCoB, via a membrane-bound heterodisulfide reductase (HdrDE), which further contributes to the proton gradient^{11,16}. Nevertheless, how electrons are diverted to the extracellular side through membrane-bound electron transport chains remains to be elucidated. Putative genes encoding MHCs in certain species of *Methanosarcina* may be critical to extracellular electron transfer. For example, *M. acetivorans* failed to donate electrons to anthraquinone-2,6-disulfonate (AQDS), a surrogate for humus, when a gene called *MmcA* encoded MHC was deleted¹⁸. AQDS also stimulates extracellular respiration with the Fe³⁺ in *M. acetivorans* by interacting with MHCs, and extracellular electron transfer can drive the generation of an ion gradient that is required for energy conservation, which thereby augments *M. acetivorans* growth^{14,19}.

In this study, we used *M. acetivorans* to study the mechanistic interaction between methanogenic archaea and humus. We found that humus respiration can promote both methylotrophic and acetoclastic methanogenesis of *M. acetivorans*. However, transcriptomic analyses demonstrated that none of the putative MHC genes were significantly regulated in humus-respiring cells, whereas a gene cluster that encodes cell surface quinoproteins was significantly upregulated. The quinone type contained in the quinoproteins was determined to be pyrroloquinoline quinone (PQQ). Electron transport assays using ferrihydrite indicated that the upregulated quinoproteins and membrane-bound MP were involved in extracellular electron transfer. Finally, the distribution of the cell surface quinoproteins was analyzed within the archaeal domain, possibly shedding light into the humus-respiratory growth of methanogens, which are ecologically implicated in the global carbon cycle.

Results

Humus respiration promotes the methylotrophic and acetoclastic methanogenesis of *M. acetivorans*

Exploration of the humus-respiring mechanism was prompted by previous findings that the surrogate for humus, AQDS, facilitates the membrane-bound electron transport chain and energy conservation in *M. acetivorans*¹⁴. We first tested how humus impacts the growth and methane production in *M. acetivorans*. The addition of 0.5 and 1 mM humus significantly enhanced methane production at the mid-log phase of cultures that were amended with either methanol or acetate as a carbon source (Figs. 1A and 1D), and the amounts of cellular protein that were cultured for 100 hours and 200 hours for methanol-grown and acetate-grown, respectively, were 2-fold greater when the medium was supplemented with humus (Figs. 1C and 1F). The enhancing effect was also confirmed by monitoring the consumption of methanol and acetate, which indicated that humus stimulated both methylotrophic and acetoclastic methanogenesis in *M. acetivorans* (Figs. 1B and 1E). Prominent and abundant coccoid-shaped *M. acetivorans* cells that were attached to humus were detected by scanning electron microscopy (Figs. 1G and 1H). In addition, FTIR analysis of the cellular surface showed peaks at $3,430\text{ cm}^{-1}$, which were ascribed to O-H stretching and were wider in cells cultured with humus than in those not cultured with humus (Extended Fig. 1A). When the humus in the medium was substituted with AQDS, we observed a reduction in AQDS accompanied by cellular growth, which validated the previous findings that the quinone groups in humus constitute the primary electron-accepting moiety (Extended Fig. 1B).

Identification of cell surface quinoproteins involved in humus respiration

To gain insights into how humus respiration stimulates methanogenic pathways, we performed transcriptomic analyses of cells that were cultured with or without humus. The differentially expressed genes were screened with univariate statistical significance ($\log_2(\text{FC}) > 1.0$ or < -1.0 , and $p < 0.05$). Among the 4,462 genes expressed in *M. acetivorans*, a total of 79 and 340 genes were upregulated in the methanol- and acetate-grown cultures with humus respiration, respectively. Totals of 60 and 16 genes were downregulated in the methanol- and acetate-grown cultures with humus respiration, respectively (Extended Fig. 2). However, none of the genes directly involved in the methanogenic pathway, such as the genes encoding methyl-CoM reductase that catalyzes the production of methane in both methylotrophic and acetoclastic methanogenesis, were significantly regulated (Extended table 1). In addition, those genes encoding membrane-bound Rnf and Fpo complexes that have been known to participate in energy conservation for the growth of *M. acetivorans*, were also not significantly regulated (Extended table 1).

Remarkably, a gene cluster ranging from *MA4284* to *MA4315* was significantly upregulated in both methanol- and acetate-grown cells with humus respiration (Fig. 2C). The gene cluster contains a total of 32 genes, 19 of which were obtained for RNA sequence reads. The remaining 13 genes were not obtained for transcript reads, consistent with the information of these genes in the NCBI database, i.e., these are pseudogenes missing a functional N- or C-terminus (Fig. 2A). A total of 17 expressed genes have

conserved N-terminal signal peptide sequences, and the predicted encoding products of these genes in the NCBI database are cell surface proteins. We are particularly interested in the cell surface proteins that were upregulated in humus-respiratory cells because close extracellular interactions between humus and *M. acetivorans* were observed. The detailed domain architectures of all expressed genes in the gene cluster are shown in Fig. 2B, and a brief overview is provided in Extended table 2. A total of 11 expressed genes (e.g., *MA4284*, *MA4290-91*, *MA4294*, *MA4297*, *MA4305*, *MA4309-10*, *MA4312*, and *MA4314-15*) were annotated as pyrroloquinoline quinone (PQQ)-binding β -propeller repeat proteins, which are composed of multiple β -propeller repeats with corresponding numbers of PQQ as cofactors and thus are also called quinoproteins²⁰. Three expressed genes (e.g., *MA4285*, *MA4289* and *MA4292*) were annotated as leucine-rich repeat (LRR) proteins, which have multiple LRR domains that are frequently involved in the formation of protein–protein interactions at the cell surface²¹. Most PQQ-binding β -propeller repeat proteins and LRR proteins contain multiple polycystic kidney disease (PKD) domains that are usually found in the extracellular segments of archaeal surface-layer proteins with ambiguous functions²². Five expressed genes (e.g., *MA4291*, *MA4305*, *MA4309*, *MA4312* and *MA4315*) contain multiple parallel beta-helix repeats (PbH1) that behave as a stack of parallel beta strands. Proteins containing PbH1 most often are enzymes with polysaccharide substrates²³. None of the above stated domains are conserved in another five expressed genes, of which *MA4293*, *MA4298* and *MA4302* were annotated as hypothetical proteins, while *MA4295* and *MA4304* were annotated as a cobaltochelate subunit and DUF4430 domain-containing protein, respectively. According to the domain composition of the gene cluster, we tentatively named the encoding products of the gene cluster cell surface quinoproteins, hereafter referred to as CSQs.

PQQ was isolated from the membrane fraction of *M. acetivorans*.

The gene cluster encoding CSQs in methanogenic archaea has not been reported to have a specific function, and it is completely unknown whether these CSQs contain PQQ as cofactors. Therefore, we followed a previously commonly used procedure for isolating quinones from the microbial membrane fraction and determined the isolated products by LC–MS based on a previously reported method^{24,25}. As illustrated in Figs. 3A-3C, our isolated products from the methanol- and acetate-grown membrane fractions exhibited the same molecular ion peaks at m/z equal to 329, 285, 241 and 197 as the PQQ standard. According to previous reports^{26,27}, the precursor ion of PQQ is m/z 329 [M-H]⁻, while the PQQ ions that were fragmented by different carboxyl groups are m/z 285 [M-H-CO₂]⁻, m/z 241 [M-H-2CO₂]⁻, and m/z 197 [M-H-3CO₂]⁻. Our results clearly indicated that PQQ does exist in the membrane fraction of *M. acetivorans*. We then quantified the relative PQQ abundances in the membrane fractions by normalizing the total peak areas of the four ions to the known concentration of the PQQ standard. Figure 3D shows that the PQQ abundances in the membranes isolated from methanol- and acetate-grown cultures respiring with humus were significantly higher than those in normal membrane fractions ($p < 0.05$ or 0.01).

Upregulated CSQs facilitated extracellular electron transfer.

Because there is no documented method to directly monitor humus reduction, we used ferrihydrite, a natural form of Fe^{3+} , as an extracellular acceptor to quantify the rates of extracellular electron transfer from normal resting cells and resting cells with upregulated CSQs. The resting cells were washed three times to remove residual humus. Figures 4B and 4C show two representative time courses for the reduction of ferrihydrite catalyzed by methanol- and acetate-grown resting cells, respectively. The electron transfer rates catalyzed by the resting cells with upregulated CSQs were ~ 2 -fold greater than those catalyzed by the same amounts of normal resting cells. Additions of 2-hydroxyphenazine (2-HP), an analog of MP, increased the rates by ~ 2 -fold when catalyzed by normal resting cells but by ~ 4 -fold when catalyzed by resting cells with upregulated CSQs, which suggested a role of 2-HP as an electron mediator to interact with CSQs. These results establish that the CSQs that are abundant on the cell surface of *M. acetivorans* facilitate extracellular electron transfer, in which MP was likely involved.

CSQs are widely distributed in methanogens

A survey within the archaeal domain retrieved 2,684 predicted PQQ-binding β -propeller repeat proteins. Intriguingly, they are primarily clustered in Halobacteria (59.2%) and methanogens (19.3%). Of particular interest, 6.7% of all PQQ-binding proteins were predicted in genus *Methanosarcina*, although only a handful of species were identified in this genus (Fig. 5A). A further search for CSQ homologous proteins in a nonredundant protein database confirmed the finding that PQQ-binding proteins are most abundant in the genus *Methanosarcina* among methanogens. For the MA4284 homologous that have multiple PQQ domains and PKD domains, 90.6% were present in the phylum Euryarchaeota, of which 62.6% are present in *Methanosarcina* (Fig. 5B). For the MA4290 homologous proteins that have only three PQQ domains, over 50% were found in the phylum Euryarchaeota, of which 34.6% were present in *Methanosarcina* (Fig. 5C). The analysis for all the other PQQ-containing CSQs were consistent with those for MA4284 and MA4290 (Extended Fig. 3). Taken together, these results clearly suggest the evolutionary enrichment of PQQ-binding and CSQ-homologous proteins in methanogens, particularly in *Methanosarcina*, which confirms the key role of PQQ in these archaeal groups.

Discussion

Figure 6 shows the proposed pathway for the methylotrophic and acetotrophic growth of *M. acetivorans* coupled with humus respiration. For methylotrophic methanogenesis, electrons are derived from the oxidation of the methyl-group in methanol. A total of 2 moles of F_{420}H_2 and 1 mole of Fd_{red} are generated from the oxidation of 4 moles of methyl groups to 1 mole of CO_2 , and F_{420}H_2 has been reported to be the primary electron donor to the membrane-bound Fpo complex, coupled with a higher H^+ gradient on the extracellular side that is required for energy conservation¹⁷. For acetoclastic methanogenesis, electrons are derived from the oxidation of the carbonyl group in acetate, and only 1 mole of Fd_{red} is generated from the oxidation of 1 mol of acetate. Fd_{red} can donate electrons to the membrane-bound Rnf complex, coupled with a higher Na^+ gradient on the extracellular side that is also required for energy conservation¹⁶. MP has been confirmed to mediate electron transfer from the Fpo or Rnf complex to the

membrane-bound Hdr in both methylotrophic and acetoclastic methanogenesis and couples with another higher H^+ gradient on the extracellular side, which thereby enhances energy conservation²⁸. Our finding that the analog of MP was able to stimulate the extracellular electron transport rate suggests that MP is likely to participate in humus respiration. Given that the redox cycling of MP inevitably drives the generation of the H^+ gradient for energy conservation, it is reasonable to speculate that MP mediates electron transport from the Rnf or Fpo complex to the CSQs for humus respiration, which significantly stimulates the methanogenic growth of *M. acetivorans* (Fig. 1).

MHCs have been proposed to play an essential role in extracellular electron transfer for AQDS reduction in *M. acetivorans*¹⁸. A total of 5 genes encoding MHCs in the genomic DNA of *M. acetivorans* were identified, and a gene (*MA0658*) called *MmcA*, which is cotranscribed with genes encoding the Rnf complex, was proposed as a major component for extracellular electron transfer to AQDS. However, only one gene (*MA2925*) annotated as cytochrome *c* peroxidase was upregulated in the acetate-grown cells respired with humus, but not in the methanol-grown cells respired with humus. Other genes were not significantly regulated in any of the humus-respiring cells. Our results indicated that MHCs may not play an essential role in extracellular electron transfer for humus respiration. It is worth noting that the predicted genes encoding MHCs are neither universal nor unique to *Methanosarcina* spp. For example, *M. barkeri*, which is also capable of extracellular electron transfer, does not contain potential MHCs^{11,29}. *M. mazei* contained only one annotated MHC, but deletion of this gene did not disrupt extracellular electron transfer²⁹. From the above evidence, it can be seen that MHCs are not an indispensable part of extracellular electron transfer in *Methanosarcina* spp.

Our studies identified a previously unexplored cell surface proteins containing PQQs, which provide a potential electrical contact with humus. As the third type of redox prosthetic cofactor after pyridine nucleotides and flavins, PQQ is a noncovalently bound amino acid-derived quinone cofactor of quinoproteins, particularly for some bacterial cytoplasmic membrane-bound dehydrogenases^{20,30}. Electron transfer between the membrane-bound quinone pools (menaquinone or ubiquinone) and PQQ-containing dehydrogenases usually plays an essential role in bacterial energy-conserving respiration³¹. Here, the electron interplay between quinone pool and PQQ was first documented in methanogenic archaea, contributing to an improved understanding for humus respiration. The membrane-bound MP, which is analogous to ubiquinone, could transfer the intracellular electrons to the CSQs containing PQQ, which is reduced to hydroquinone form (PQQH₂), and in doing so donates the two sequential electrons to the quinone groups in humus by way of free radical semiquinone. The redox potential of PQQ has been determined to be approximately + 90 mV, which is likely to be influenced by its environment in the quinoproteins³². Given that the redox potential of MP (e.g., - 165 mV) is much more negative than that of PQQ, electrons are likely to be transferred from MP to CSQs with PQQ, as proposed in Fig. 6. Two previous studies have found clues that quinones may be involved in extracellular electron transfer in *Methanosarcina* spp. One study showed that the genes encoding PQQ-containing quinoproteins were significantly upregulated in *M. barkeri* cells grown via direct interspecies electron transfer³³, and a second study showed that humic-like compounds were secreted by *M. barkeri* to facilitate extracellular electron

transfer³⁴. Here, we first demonstrated that PQQ was indeed present in the membrane fraction of *M. acetivorans*, and the abundance of PQQ was higher in humus-respiring cells, which is consistent with the transcriptomic analysis. Notably, two genes (e.g., *MA3035* and *MA4279*) annotated as coenzyme PQQ synthesis protein E are present in the genomic DNA of *M. acetivorans*, which indicates that biosynthesis of PQQ in *M. acetivorans* is possible.

Ecological implications

Microbial humus respiration is ecologically implicated in the decomposition of natural and contaminant organics in diverse anaerobic environments. Humus-respiratory growth of nonmethanogenic bacteria has been confirmed, which accounts for CO₂ emissions during the anaerobic decomposition of organics^{10,35}. However, whether methanogenic archaea being capable of performing humus-respiratory growth is ambiguous. A traditional view has emerged that methanogenic growth and humus-respiratory growth are competitive processes for energy conservation due to the evidence that quinone reduction inhibited methanogenesis^{36,37}. Our work has updated this view by demonstrating that methanogenic growth can be coupled with humus-respiratory growth, which may play an important role in the context of global methane dynamics.

The distribution analysis suggests that CSQ homologous proteins are most abundant in the genus *Methanosarcina* among methanogens, which is the one of two genera that are currently known to perform acetoclastic methanogenesis, accounting for approximately two-thirds of the one billion metric tons of methane produced annually in Earth's anaerobic environments. The CSQs were found in all intensively investigated *Methanosarcina* spp. including *M. acetivorans*, *M. barkeri*, *M. mazei*, and *M. thermophila*, which were isolated from biomass-rich marine or freshwater sediments, where they inevitably interact directly with humus. The newly proposed extracellular electron transfer pathway based on CSQs fills the current knowledge gap concerning the mechanism by which humus-respiratory growth occurs in *Methanosarcina*. In addition, genera *Methanosarcina* is phylogenetically related to certain clades of anaerobic methanotrophic archaea (e.g., ANME-2a and ANME-2d)³⁸, which perform anaerobic oxidation of methane by coupling with extracellular reduction of electron acceptors. Considering that the CSQs are also widely distributed in ANME-2 clades (Fig. 5), our finding predicts a significant role of CSQs in the anaerobic methane cycle in sediments across the globe.

Methods

Organism and growth conditions

M. acetivorans C2A was purchased from the Japan Collection of Microorganisms (JCM, Japan) and was cultivated under strict anaerobic conditions at 37°C in a high-salt medium, as previously reported³⁹. Methanol that was passed through a 0.22 µm filter was added to provide a final concentration of 125 mM and was used as the methanol-grown substrate. An autoclaved acetate sodium solution was added

to provide a final concentration of 90 mM and was employed as the acetate-grown substrate. The cultures were separately inoculated at ratios of 1:100 and 1:10 with methanol-grown and acetate-grown precultures, respectively, and incubated at 37°C in the dark without shaking. Humus was purchased from Shanghai Yuanye Biotechnology Co., Ltd. The indicated concentrations of anaerobic humus were added to the medium using a syringe immediately before inoculation.

Analytical techniques for growth parameters

The production of methane and total cellular protein concentrations were measured as previously reported³⁹. The methanol concentrations were measured by a gas chromatograph (GC-2014, Shimadzu, Japan) equipped with a DB-FFAP column (internal diameter, 0.32 mm; length, 30 m) and a flame ionization detector. The cultures that were collected at various time points were centrifuged at 5,000×g for 20 min to separate the medium from the cell pellet. The supernatant was collected, passed through a 0.22 μm filter and was then used in the assays. High-purity nitrogen was used as the carrier gas at a flow rate of 3.77 mL/min. The run time was 10.44 min, and the detector temperature was 225°C. The sodium acetate concentrations were determined by an HPLC system (LC-20A, Shimadzu, Japan) equipped with a Hypersil GOLD™ aQ column and UV–VIS detector. The supernatant was passed through a 0.22 μm filter and acidified with 0.1 M H₂SO₄. The column temperature was 40°C. (NH₄)₂PO₄ was used as the mobile phase at a flow rate of 1 mL/min. The run time was 8 min.

Transcriptomic analysis

Cells cultured at the mid-log phase in triplicate were collected by centrifugation at 5,000×g for 20 min at 4°C. Total RNA was extracted using TRIzol reagent (Invitrogen, USA) as previously described⁴⁰. A directional library was prepared by using the Truseq™ stranded RNA sample prep kit (Illumina, USA). mRNA was sequenced using a NovaSeq 6000 sequencer (Illumina, USA) at Biozeron Co., Ltd (Shanghai, China). All raw sequencing data were quality checked and filtered as previously described⁴¹. All reads matching the 16S and 23S rRNA genes were removed, and the remaining reads were then used to map against the published genome of *M. acetivorans* C2A (NC_003552.1). The mapped reads were normalized to the numbers of reads per kilobase per million reads (rpkm), as previously reported⁴².

Determination of PQQ isolated from the membrane fraction

Extraction of PQQ from the membrane was performed based on an amended isooctane extraction method^{24,25}. Lyophilized cell membranes were first prepared. Cells that were cultured up to the late exponential phase were harvested by centrifugation at 5,000×g and 4°C for 20 min. The supernatant was discarded, and the pellet was washed twice using Tris buffer (pH 7.5). Then, the cell pellet was resuspended in 20 mL of Tris buffer with ultrasonication. The unbroken cells and debris were eliminated by centrifugation at 4,000×g for 10 min. The membranes were obtained by centrifugation at 120,000×g at 4°C for 2 h and resuspended in Tris buffer with an appropriate volume. The concentrations of the membrane proteins were determined with a BCA protein assay kit (Jiancheng Bioengineering Institute, China). The membrane fraction was then vacuum freeze-dried for PQQ extraction.

The lyophilized cell membranes were immediately resuspended in 20 mL of isooctane and extracted with continuous stirring at room temperature for 3 h. The supernatant was removed, after which fresh isooctane was added to the pellet for a second extraction overnight. After a third extraction for 24 h, the isooctane was discarded from the suspension, and the pellet was completely dried in a vacuum oven. The dried pellet was resuspended in 2 mL of methanol and passed through a 0.22 µm filter. The PQQ standard was pretreated in the same manner. PQQ isolated from the membrane fraction and the PQQ standard were analyzed by LC–MS (Thermo UltiMate 3000 for HPLC and Thermo LCQ fleet for MS). A total of 5 µL of the sample was autoinjected into the HPLC system in which methanol and water were used as the mobile phases (v:v = 6:4) at a flow rate of 0.2 mL/min. The column temperature was 40°C, and the column eluent was sent to an ion trap mass spectrometer. Product ion scanning was conducted under electrospray ionization in a positive mode at 320°C.

Electron transport assays.

All electron transport assays were performed in serum-stopped glass vials with a 100% N₂ atmosphere. The electron transport activity from the resting cells to ferrihydrite (Fe³⁺) was assayed by monitoring the generation of Fe²⁺ that chelated with ferrozine, forming a magenta complex with a maximum absorbance at 562 nm. The resting cells were washed three times with medium to remove residual humus. The standard reaction mixture (10 mL) contained 1.6×10⁸ CFU/mL of resting cells and 100 µM 2-HP. Ferrihydrite was added to start the reaction at a final concentration of 1.25 mM. A total of 50 µL of the reaction mixture was collected at various time points and reacted with ferrozine solution for the absorbance assay.

SEM and FTIR analyses

A total of 10 mL of cells that were cultured at the mid-log phase were harvested by centrifugation at 5,000×g for 10 min. The supernatant was discarded, and the cell pellet was washed twice and analyzed by SEM and FTIR as described elsewhere³⁹.

Phylogenies analysis and distribution patterns of CSQs in Archaea

The representative species and 16S rRNA gene sequences were obtained from the GTDB (Genome Taxonomy Database) and Silva (high quality ribosomal RNA database) databases. The phylogenetic trees of the 16S rDNA sequences were constructed by using the maximum likelihood method in MEGA 7.0. The sequences of the PQQ domain-containing proteins were downloaded from the SMART (Simple Modular Architecture Research Tool) database. The putative CSQ homologs were found by performing BLAST analysis from the nonredundant (NR) protein database. The proteins were clustered with USEARCH with a 95% similarity threshold to remove redundant proteins present in the protein databases. The cluster centroids and cluster members not from the same species of centroids were retained for further analysis.

References

1. Hayes, M. Humus Chemistry - Genesis, Composition, Reactions - Stevenson, F.J. *Nature* **303**, 835–836 (1983).
2. Lipczynska-Kochany, E. Humic substances, their microbial interactions and effects on biological transformations of organic pollutants in water and soil: A review. *Chemosphere* **202**, 420–437 (2018).
3. Lovley, D.R., Coates, J.D., Blunt-Harris, E.L., Phillips, E.J.P. & Woodward, J.C. Humic substances as electron acceptors for microbial respiration. *Nature* **382**, 445–448 (1996).
4. Lovley, D.R. et al. Humic substances as a mediator for microbially catalyzed metal reduction. *Acta Hydrochimica Et Hydrobiologica* **26**, 152–157 (1998).
5. Scott, D.T., McKnight, D.M., Blunt-Harris, E.L., Kolesar, S.E. & Lovley, D.R. Quinone moieties act as electron acceptors in the reduction of humic substances by humics-reducing microorganisms (vol 32, pg 2984, 1998). *Environmental Science & Technology* **33**, 372–372 (1999).
6. Shi, L. et al. Extracellular electron transfer mechanisms between microorganisms and minerals. *Nature Reviews Microbiology* **14**, 651–662 (2016).
7. Lovley, D.R., Fraga, J.L., Coates, J.D. & Blunt-Harris, E.L. Humics as an electron donor for anaerobic respiration. *Environmental Microbiology* **1**, 89–98 (1999).
8. Roden, E.E. et al. Extracellular electron transfer through microbial reduction of solid-phase humic substances. *Nature Geoscience* **3**, 417–421 (2010).
9. Klupfel, L., Piepenbrock, A., Kappler, A. & Sander, M. Humic substances as fully regenerable electron acceptors in recurrently anoxic environments. *Nature Geoscience* **7**, 195–200 (2014).
10. Valenzuela, E.I. & Cervantes, F.J. The role of humic substances in mitigating greenhouse gases emissions: Current knowledge and research gaps. *Science of the Total Environment* **750**(2021).
11. Gao, K.L. & Lu, Y.H. Putative Extracellular Electron Transfer in Methanogenic Archaea. *Frontiers in Microbiology* **12**(2021).
12. Wang, H. et al. Redox cycling of Fe(II) and Fe(III) in magnetite accelerates acetoclastic methanogenesis by *Methanosarcina mazei*. *Environmental Microbiology Reports* **12**, 97–109 (2020).
13. Fu, L. et al. NanoFe₃O₄ as Solid Electron Shuttles to Accelerate Acetotrophic Methanogenesis by *Methanosarcina barkeri*. *Frontiers in Microbiology* **10**(2019).
14. Prakash, D., Chauhan, S.S. & Ferry, J.G. Life on the thermodynamic edge: Respiratory growth of an acetotrophic methanogen. *Science Advances* **5**(2019).
15. Kulkarni, G., Mand, T.D. & Metcalf, W.W. Energy Conservation via Hydrogen Cycling in the Methanogenic Archaeon *Methanosarcina barkeri*. *Mbio* **9**(2018).
16. Ferry, J.G. *Methanosarcina acetivorans*: A Model for Mechanistic Understanding of Acetoclastic and Reverse Methanogenesis. *Frontiers in Microbiology* **11**(2020).

17. Welte, C. & Deppenmeier, U. Bioenergetics and anaerobic respiratory chains of acetoclastic methanogens. *Biochimica Et Biophysica Acta-Bioenergetics* **1837**, 1130–1147 (2014).
18. Holmes, D.E. et al. A Membrane-Bound Cytochrome Enables *Methanosarcina acetivorans* To Conserve Energy from Extracellular Electron Transfer. *Mbio* **10**(2019).
19. Yan, Z., Joshi, P., Gorski, C.A. & Ferry, J.G. A biochemical framework for anaerobic oxidation of methane driven by Fe(III)-dependent respiration. *Nature Communications* **9**(2018).
20. Duine, J.A. & Jongejans, J.A. Quinoproteins, Enzymes with Pyrrolo-Quinoline Quinone as Cofactor. *Annual Review of Biochemistry* **58**, 403–426 (1989).
21. Kobe, B. & Kajava, A.V. The leucine-rich repeat as a protein recognition motif. *Current Opinion in Structural Biology* **11**, 725–732 (2001).
22. Jing, H. et al. Archaeal surface layer proteins contain beta propeller, PKD, and beta helix domains and are related to metazoan cell surface proteins. *Structure* **10**, 1453–1464 (2002).
23. Jenkins, J., Mayans, O. & Pickersgill, R. Structure and evolution of parallel beta-helix proteins. *Journal of Structural Biology* **122**, 236–246 (1998).
24. Takamiya, K. & Nishimura, M. Dual Roles of Ubiquinone as Primary and Secondary-Electron Acceptors in Light-Induced Electron-Transfer in Chromatophores of *Chromatium-D*. *Plant and Cell Physiology* **16**, 1061–1072 (1975).
25. Ding, H.G., Robertson, D.E., Daldal, F. & Dutton, P.L. Cytochrome-Bc1 Complex [2Fe-2S] Cluster and Its Interaction with Ubiquinone and Ubihydroquinone at the Q0 Site - a Double-Occupancy Q0 Site Model. *Biochemistry* **31**, 3144–3158 (1992).
26. Kato, C. et al. Determination of pyrroloquinoline quinone by enzymatic and LC-MS/MS methods to clarify its levels in foods. *Plos One* **13**(2018).
27. Noji, N. et al. Simple and sensitive method for pyrroloquinoline quinone (PQQ) analysis in various foods using liquid chromatography/electrospray-ionization tandem mass spectrometry. *Journal of Agricultural and Food Chemistry* **55**, 7258–7263 (2007).
28. Abken, H.J. et al. Isolation and characterization of methanophenazine and function of phenazines in membrane-bound electron transport of *Methanosarcina mazei* Gol. *Journal of Bacteriology* **180**, 2027–2032 (1998).
29. Yee, M.O. & Rotaru, A.E. Extracellular electron uptake in *Methanosarcinales* is independent of multiheme c-type cytochromes. *Scientific Reports* **10**(2020).
30. Matsutani, M. & Yakushi, T. Pyrroloquinoline quinone-dependent dehydrogenases of acetic acid bacteria. *Applied Microbiology and Biotechnology* **102**, 9531–9540 (2018).
31. Qin, Z.J., Yu, S.Q., Chen, J. & Zhou, J.W. Dehydrogenases of acetic acid bacteria. *Biotechnology Advances* **54**(2022).
32. Anthony, C. Pyrroloquinoline quinone (PQQ) and quinoprotein enzymes. *Antioxidants & Redox Signaling* **3**, 757–774 (2001).

33. Holmes, D.E. et al. Electron and Proton Flux for Carbon Dioxide Reduction in *Methanosarcina barkeri* During Direct Interspecies Electron Transfer. *Frontiers in Microbiology* **9**(2018).
34. Huang, L.Y. et al. Light-driven carbon dioxide reduction to methane by *Methanosarcina barkeri* in an electric syntrophic coculture. *Isme Journal* (2021).
35. Keller, J.K., Weisenhorn, P.B. & Megonigal, J.P. Humic acids as electron acceptors in wetland decomposition. *Soil Biology & Biochemistry* **41**, 1518–1522 (2009).
36. Cervantes, F.J., van der Velde, S., Lettinga, G. & Field, J.A. Competition between methanogenesis and quinone respiration for ecologically important substrates in anaerobic consortia. *Fems Microbiology Ecology* **34**, 161–171 (2000).
37. Cervantes, F.J. et al. Contribution of quinone-reducing microorganisms to the anaerobic biodegradation of organic compounds under different redox conditions. *Biodegradation* **19**, 235–246 (2008).
38. Timmers, P.H. et al. Reverse Methanogenesis and Respiration in Methanotrophic Archaea. *Archaea* 2017, 1654237 (2017).
39. Song, Y.X. et al. Nano zero-valent iron harms methanogenic archaea by interfering with energy conservation and methanogenesis. *Environmental Science-Nano* **8**, 3643–3654 (2021).
40. Shrestha, P.M. et al. Syntrophic growth with direct interspecies electron transfer as the primary mechanism for energy exchange. *Environmental Microbiology Reports* **5**, 904–910 (2013).
41. Rotaru, A.E. et al. A new model for electron flow during anaerobic digestion: direct interspecies electron transfer to *Methanosaeta* for the reduction of carbon dioxide to methane. *Energy & Environmental Science* **7**, 408–415 (2014).
42. Holmes, D.E. et al. Metatranscriptomic Evidence for Direct Interspecies Electron Transfer between *Geobacter* and *Methanotrix* Species in Methanogenic Rice Paddy Soils. *Applied and Environmental Microbiology* **83**(2017).

Declarations

Acknowledgments

The authors thank Sen Wang from State Key laboratory of Microbial Technology of Shandong University for help and guidance in SEM. The authors thank Wenshan Qi from Biozeron Co., Ltd. for his technical assistance of RNA-Seq in this study. This work was supported by National Natural Science Foundation of China (22008142), Natural Science Foundation of Jiangsu Province (BK20200232) and Qilu Youth Talent Program of Shandong University.

Author contributions: Z.Y., Y.S. and J.F. conceived and designed the study; Y.S., K.D., L.L. and F.Z. performed the experiment and collected the data; Z.Y., Y.S., L.L. and M.W. wrote the manuscript; J.F., M.W. and S.W. analyzed and interpreted the data; C.S., X.Y., M.W. and S.W. revised the manuscript.

Competing interests: The authors declare that they have no competing interests.

Figures

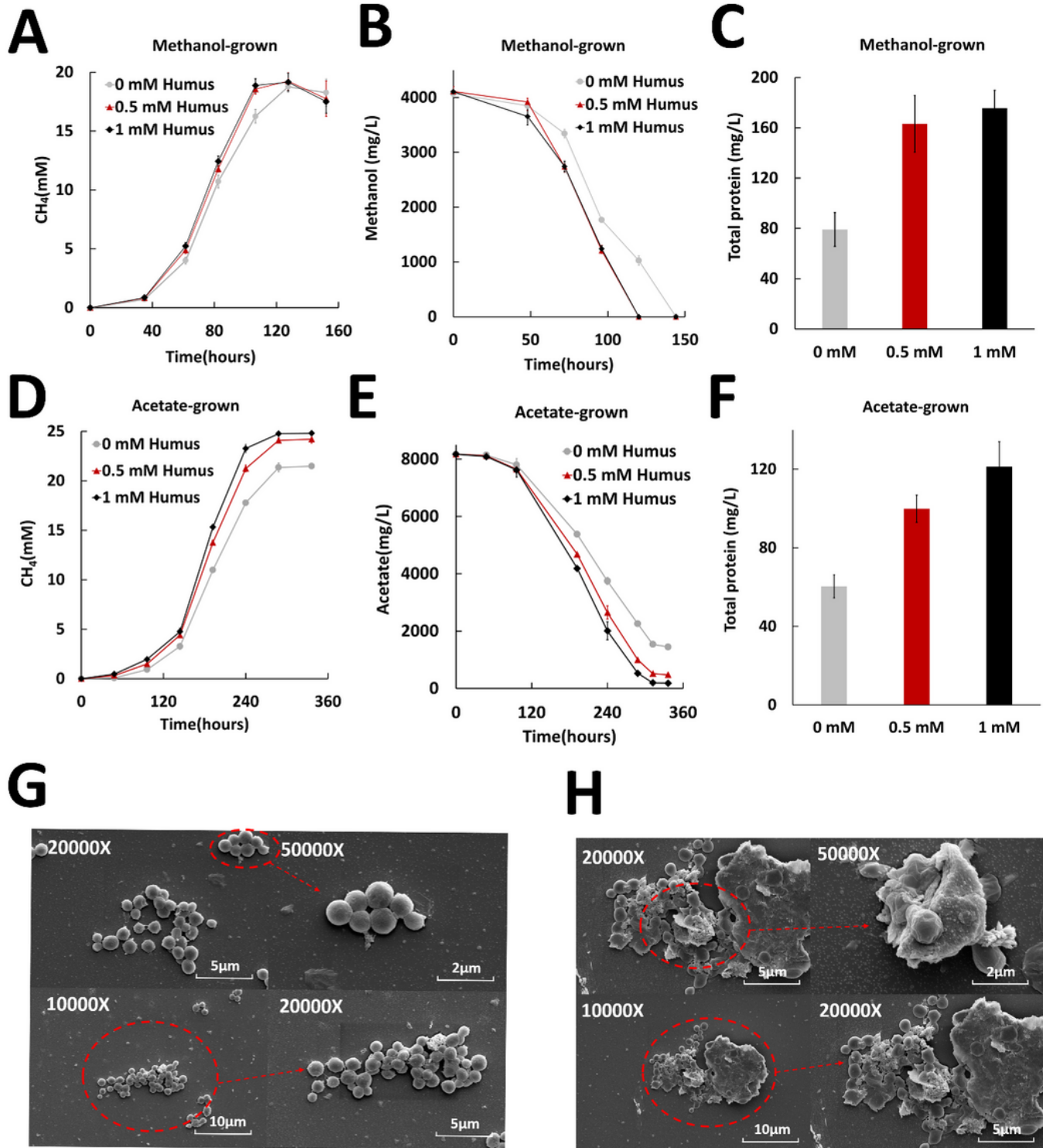


Figure 1

Growth parameters and SEM analysis of *M. acetivorans* grown with or without humus. Time-dependent methane production of methanol-grown cultures (A) and acetate-grown cultures (D). Time-dependent carbon source utilization of methanol-grown cultures (B) and acetate-grown cultures (E). Total cellular

proteins grown for 100 hours and 200 hours in methanol-grown cultures (C) and acetate-grown cultures (F), respectively. SEM pictures of *M. acetivorans* cells without (G) and with (H) humus. Magnification and scale bars are shown in each of the SEM pictures.

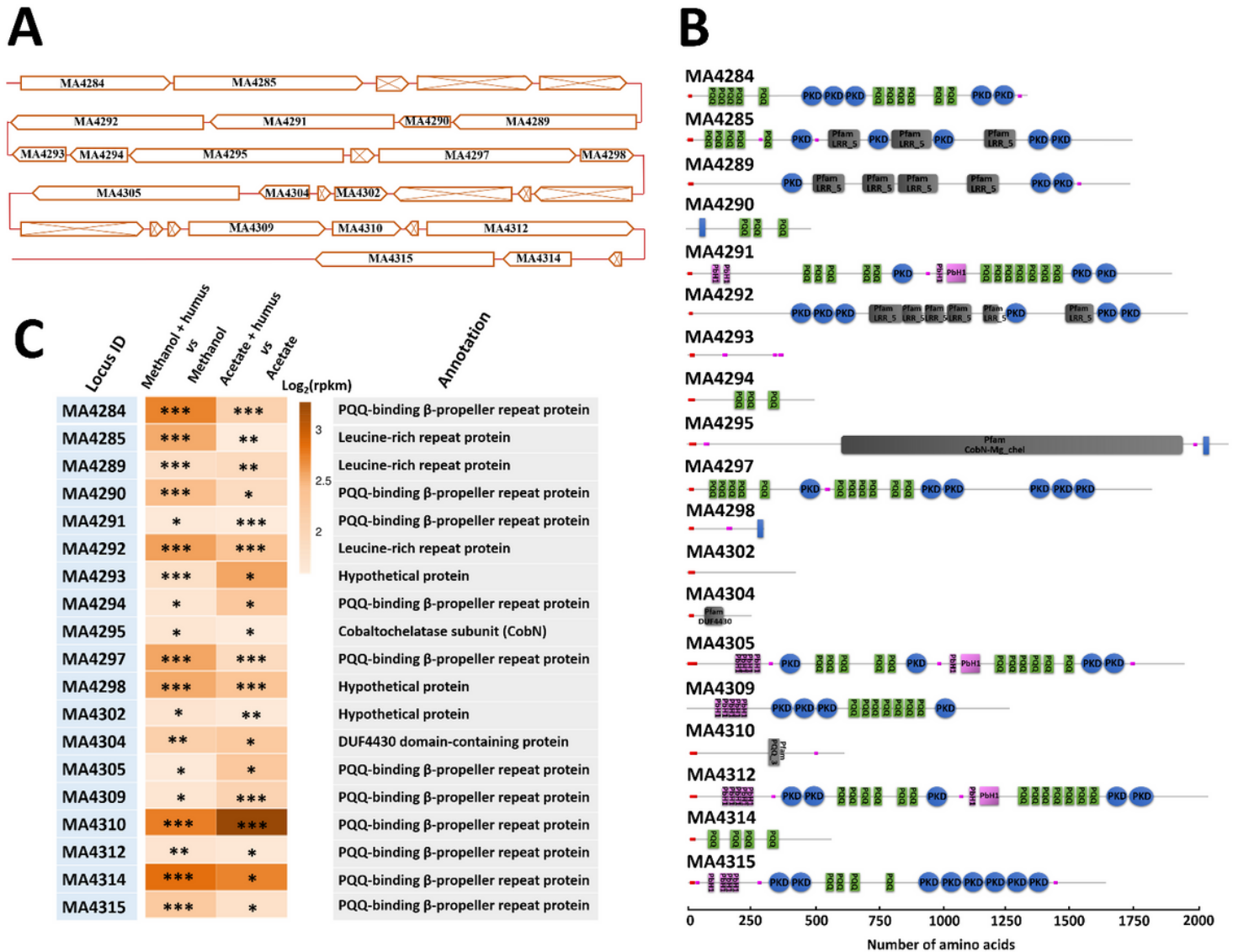


Figure 2

A gene cluster encoding CSQs was upregulated in *M. acetivorans* undergoing respiratory growth with humus. (A) Arrangement of the gene cluster encoding CSQs. The genes labeled with cross marks are pseudogenes in which the N- or C- terminus is disordered. (B) Domain architectures of the gene cluster encoding CSQs analyzed by the Simple Modular Architecture Research Tool. Red box in the N-terminus indicates signal peptides. Pink box indicates regions of low compositional complexity. PQQ indicates beta-propeller repeat domain with PQQ as a cofactor. PKD indicates polycystic kidney disease domain. PpH1 indicates parallel beta-helix repeat domain. LRR indicates leucine-rich repeat domain. CobN-

Mg_chel indicates magnesium cobaltochelate. DUF4430 indicates domain of unknown function 4430. (C) Heatmap analysis of the transcript abundances of the gene cluster encoding CSQs from triplicate independent cultures presented as \log_2 (rpkm) values (reads per kilobase per million mapped reads). The differences were considered significant at $p < 0.05$. * indicates $p < 0.05$; ** indicates $p < 0.01$; *** indicates $p < 0.005$.

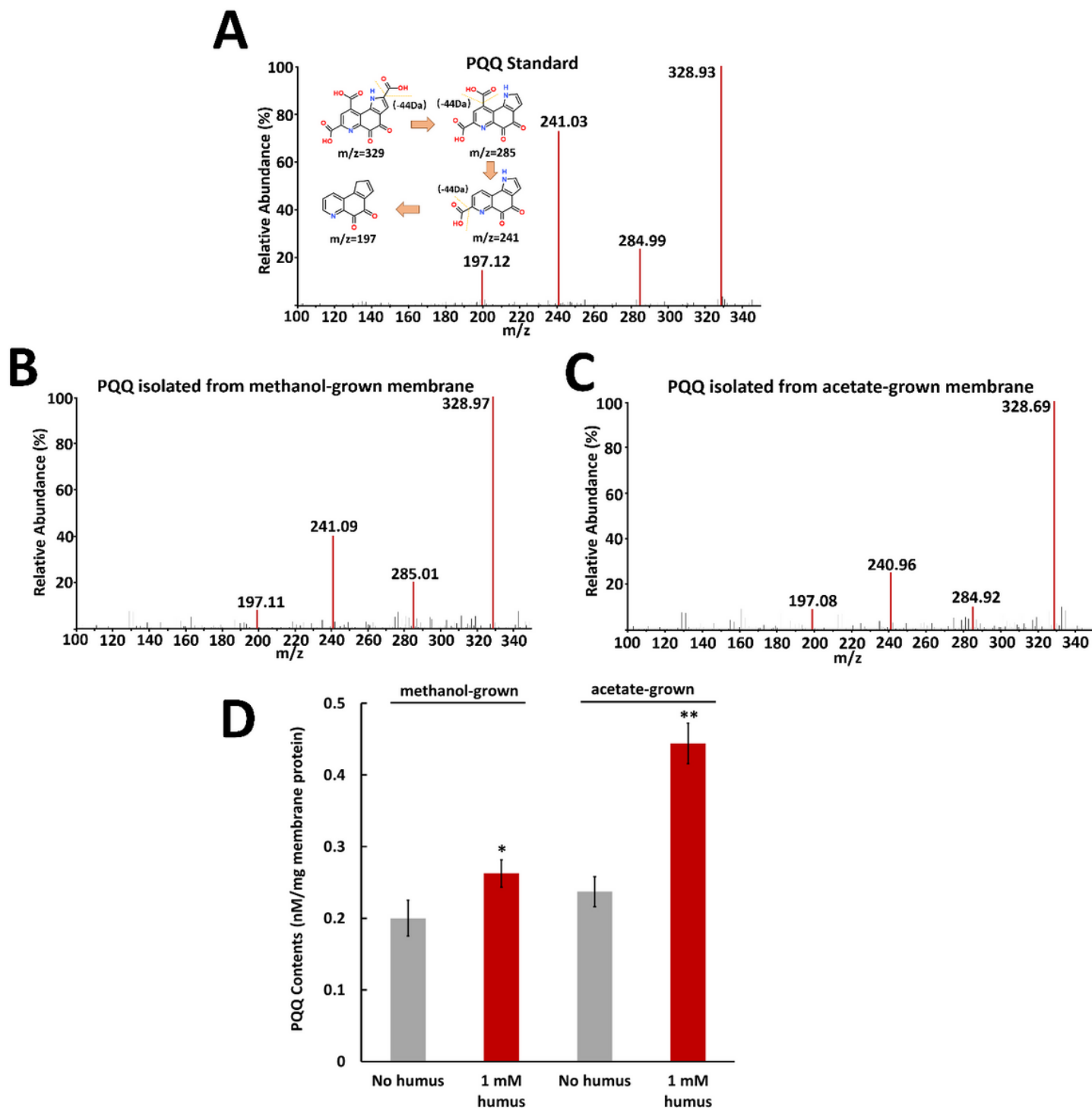


Figure 3

Isolation of PQQ from the membrane fraction of *M. acetivorans* and analysis by LC–MS. (A) Ion mass spectrum of standard PQQ. The inset shows the proposed fragmentation pattern of PQQ. (B) Ion mass spectrum of isolated PQQ from the methanol-grown membrane. (C) Ion mass spectrum of isolated PQQ from the acetate-grown membrane. (D) Quantification of isolated PQQ from the membranes separated from methanol- and acetate-grown respiratory cultures with or without humus. * and ** indicate significant differences between the control and humus treatments at $p < 0.05$ and 0.01 , respectively.

Figure 4

The upregulated CSQs are involved in extracellular electron transfer. (A) Schematic diagram for the electron transport to ferrihydrite (Fe^{3+}) from normal resting cells and resting cells with upregulated CSQs. (B) Ferrihydrite reduction by methanol-grown cells. (C) Ferrihydrite reduction by acetate-grown cells. The Fe^{2+} generations were monitored at an absorbance wavelength of 562 nm. Approximately 1.6×10^8 CFU/mL resting cells were used for all assays. All experiments were repeated three times, and the representative time-course results are shown here.

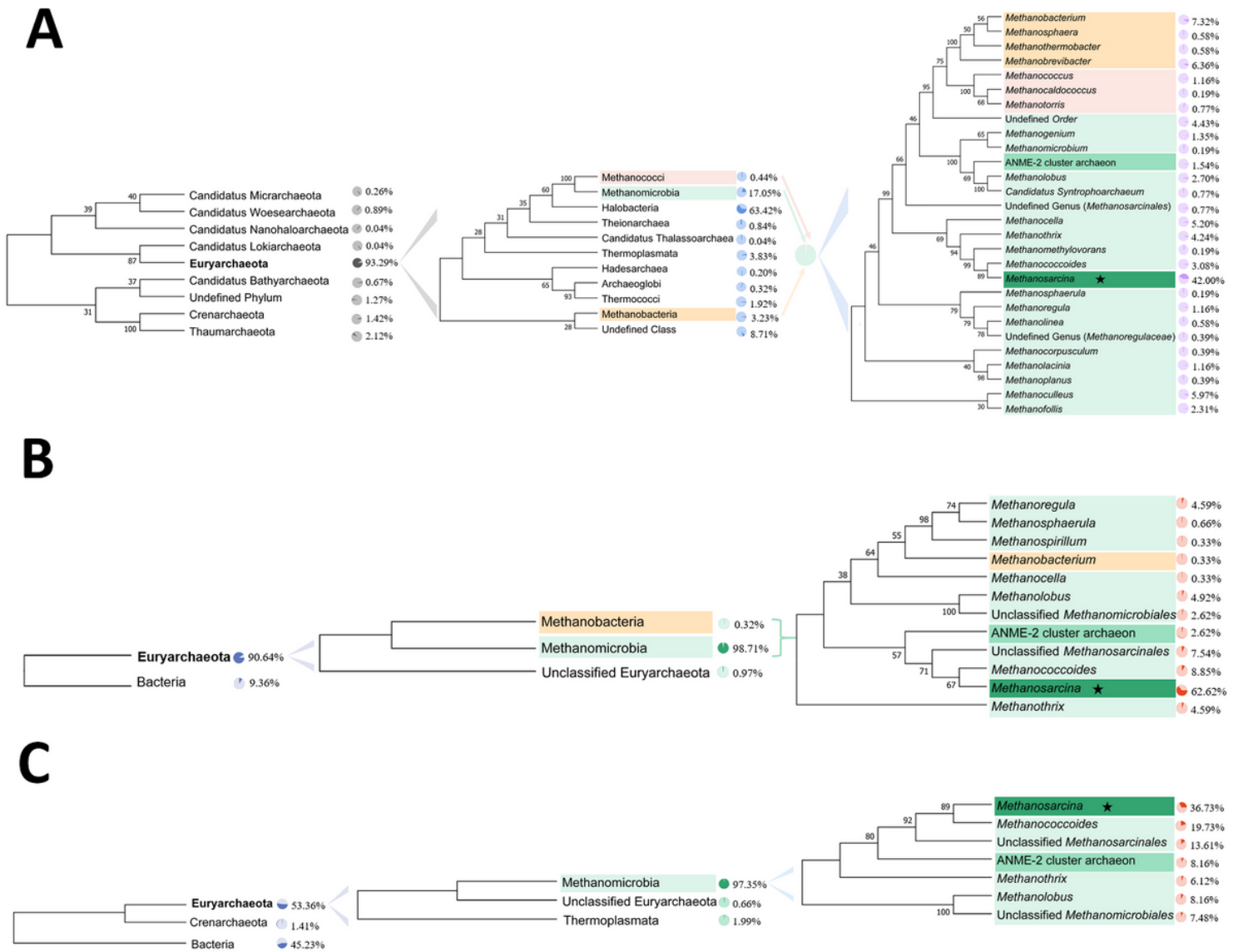


Figure 5

Prevalence of PQQ-binding β -propeller repeat proteins and predicted CSQs homologues. (A) PQQ-binding β -propeller repeat proteins; **(B)** Predicted MA4284 homologues; **(C)** Predicted MA4290 homologues. Percentage numbers indicate the percentage of targeted protein among the retrieved proteins. Number on nodes indicated bootstrap values.

